Developmental Cell
Article

A Critical Function for the Actin Cytoskeleton in Targeted Exocytosis of Prefusion Vesicles during Myoblast Fusion

Sangjoon Kim,[1,2] Khurts Shilagardi,[1,2] Shiliang Zhang,[1,2] Sabrina N. Hong,[1] Kristin L. Sens,[1] Jinyan Bo,[1] Guillermo A. Gonzalez,[1] and Elizabeth H. Chen[1,*]
[1] Department of Molecular Biology and Genetics, Johns Hopkins University School of Medicine, Baltimore, MD 21205, USA
[2] These authors contributed equally to this work.
*Correspondence: echen@jhmi.edu
DOI 10.1016/j.devcel.2007.02.019

SUMMARY

Myoblast fusion is an essential step during muscle differentiation. Previous studies in *Drosophila* have revealed a signaling pathway that relays the fusion signal from the plasma membrane to the actin cytoskeleton. However, the function for the actin cytoskeleton in myoblast fusion remains unclear. Here we describe the characterization of *solitary* (*sltr*), a component of the myoblast fusion signaling cascade. *sltr* encodes the *Drosophila* ortholog of the mammalian WASP-interacting protein. Sltr is recruited to sites of fusion by the fusion-competent cell-specific receptor Sns and acts as a positive regulator for actin polymerization at these sites. Electron microscopy analysis suggests that formation of F-actin-enriched foci at sites of fusion is involved in the proper targeting and coating of prefusion vesicles. These studies reveal a surprising cell-type specificity of Sltr-mediated actin polymerization in myoblast fusion, and demonstrate that targeted exocytosis of prefusion vesicles is a critical step prior to plasma membrane fusion.

INTRODUCTION

Cell-cell fusion is critical to the development and physiology of multicellular organisms, and is involved in a variety of biological processes such as fertilization, myogenesis, placenta development, bone remodeling, immune response, tumor metastasis, and aspects of stem cell-mediated tissue regeneration (reviewed by Chen and Olson, 2005). Thus, a mechanistic understanding of this process is not only important for fundamental biology but may also provide a basis for its manipulation in therapeutic settings.

Compared to our understanding of intracellular organelle fusion and virus-cell fusion, much less is known about the underlying mechanisms of cell-cell fusion. Recent studies in the genetically amenable fruit fly *Drosophila* have begun to provide significant insights into this process (reviewed by Abmayr et al., 2003; Chen and Olson, 2004). In *Drosophila* embryos, development of the segmentally repeated somatic muscles requires fusion between muscle founder cells and fusion-competent myoblasts. While different subsets of founder cells express different selector genes, all fusion-competent cells are specified by a single transcription factor, Lame duck (Lmd)/Myoblast incompetent (Duan et al., 2001; Ruiz-Gomez et al., 2002). During myoblast fusion, muscle founder cells attract the surrounding fusion-competent cells, which recognize, attach, and fuse with founder cells to form multinucleated syncytia. Following syncytia formation, the nucleus of the fusion-competent cell adopts the same transcriptional profile as that of the founder cell with which it has fused. Myoblast fusion takes place in two phases, with the first phase yielding bi- or trinucleated muscle precursors, followed by a second phase of additional rounds of fusion that give rise to muscle fibers with distinct sizes (Rau et al., 2001). At the ultrastructural level, myoblast fusion involves several characteristic steps (Doberstein et al., 1997). Upon cell adhesion, paired vesicles with an electron-dense margin form along the juxtaposed plasma membranes between founder and fusion-competent cells. These vesicles then presumably resolve into elongated electron-dense plaques along the apposing membranes, followed by the formation of membrane discontinuity (fusion pores), which ultimately leads to the complete fusion of the two cells. The importance of these intermediate structures (vesicles, plaques, and pores) in myoblast fusion is highlighted by the observation that various mutants arrest fusion at different steps along this path (Doberstein et al., 1997).

Further insights into the molecular mechanisms of myoblast fusion came from the elucidation of a signaling cascade from transmembrane receptors to the actin cytoskeleton (reviewed by Abmayr et al., 2003; Chen and Olson, 2004). In founder cells, two immunoglobulin (Ig) domain-containing transmembrane receptors, Dumbfounded (Duf)/Kirre and Roughest (Rst)/IrreC, are expressed and play redundant roles during myoblast fusion (Ruiz-Gomez et al., 2000; Strunkelnberg et al., 2001). Two parallel pathways mediate signal transduction from the fusion receptors to the cytoskeleton. First, a founder cell-specific

adaptor protein Antisocial (Ants)/Rols7 physically links Duf and the cytoskeleton-associated protein Myoblast city (Mbc) (Chen and Olson, 2001; Menon and Chia, 2001; Rau et al., 2001). Mbc, as its human ortholog DOCK180, likely functions as a guanine nucleotide exchange factor (GEF) for the small GTPase Rac (Brugnera et al., 2002; Erickson et al., 1997). Consistent with this, *Drosophila* Rac is essential for myoblast fusion (Hakeda-Suzuki et al., 2002). A second pathway downstream of the Duf receptor involves Loner, a different GEF, and its target, the small GTPase Arf6 (Chen et al., 2003). The Loner-Arf6 module is required for the proper localization of Rac, thus converging into the Ants → Mbc → Rac pathway at the level of Rac (Chen et al., 2003). Signal transduction in fusion-competent cells is relatively less characterized. Two fusion-competent cell-specific receptors, Sticks and stones (Sns) and Hibris (Hbs), have been identified (Artero et al., 2001; Bour et al., 2000; Dworak et al., 2001). However, intracellular proteins that mediate signal transduction from membrane receptors to the actin cytoskeleton in fusion-competent cells have yet to be uncovered.

The Wiskott-Aldrich syndrome protein (WASP) family of proteins, including WASP, neural-WASP (N-WASP), and WASP family verprolin homologs (WAVEs) 1–3, are important regulators of the actin cytoskeleton (reviewed by Miki and Takenawa, 2003). In mammalian cells, binding of the small GTPase Cdc42 activates WASPs by releasing them from an autoinhibitory conformation. WAVEs, on the other hand, are activated by Rac, another Rho family small GTPase. Both WASPs and WAVEs feed into the Arp2/3 complex, a direct regulator of actin polymerization (reviewed by Stradal and Scita, 2006). Previous studies in *Drosophila* have implicated the Mbc → Rac → WAVE pathway in myoblast fusion, as mutations in *mbc*, *rac*, or the WAVE-associated protein Kette result in myoblast fusion defects (Hakeda-Suzuki et al., 2002; Rushton et al., 1995; Schroter et al., 2004). However, the precise role of the actin cytoskeleton in myoblast fusion remains mysterious. Specifically, how could organization of the intracellular actin cytoskeleton affect plasma membrane dynamics and fusion?

In this paper, we describe the characterization of a component of the myoblast fusion signaling cascade. This component, which we named Solitary (Sltr), is the *Drosophila* ortholog of the human WASP-interacting protein (WIP). We show that Sltr is a fusion-competent cell-specific protein that is recruited to sites of fusion by the transmembrane receptor Sns. Sltr is a positive regulator of actin polymerization and is required for F-actin accumulation at sites of fusion. Electron microscopy analysis suggests that the actin cytoskeleton is involved in targeted exocytosis of prefusion vesicles at sites of fusion, thus revealing a critical step prior to plasma membrane merger.

RESULTS

Myoblast Fusion Defect in *sltr* Mutant

The *solitary* (*sltr*) allele *S1946* was isolated in a genetic screen for fusion-defective mutants. Homozygous *sltr* mutant embryos contain many mononucleated myosin heavy chain (MHC)-positive myocytes (Figures 1A and 1B). This lack-of-fusion phenotype is further confirmed by electron microscopy, which reveals myoblast clusters containing single founder cells surrounded by multiple unfused competent cells (see Figure S1 in the Supplemental Data available with this article online). Dmef2, which marks the nuclei of all somatic muscle cells (Lilly et al., 1994; Nguyen et al., 1994), is similarly expressed in wild-type and *sltr* embryos, suggesting that muscle cell fate is properly specified in *sltr* embryos (Figures 1H and 1I). Thus, the fusion phenotype of *sltr* embryos does not result from a secondary consequence of defective muscle cell fate determination. In late-stage embryos, unfused myoblasts are seen attached to elongated muscle precursors (Figures 1D and 1E), suggesting that the *sltr* mutation does not affect the recognition or adhesion between founder and fusion-competent cells, but blocks a later step in myoblast fusion.

Myoblast fusion takes place in two phases, with the first phase yielding bi- or trinucleated muscle precursors, followed by a second phase of additional rounds of fusion that give rise to muscle fibers with distinct sizes (Rau et al., 2001). To determine which phase of fusion is defective in *sltr* embryos, we examined the expression of two transcription factors, Krüppel (Kr) and Even skipped (Eve), which mark different subsets of muscle founder cells (Carmena et al., 1998; Ruiz-Gomez and Bate, 1997). In wild-type embryos, Kr staining is initially detected in bi- or trinucleated muscle precursors at stage 13 (Figure 1J), evolves into multinucleated clusters at stage 14 (Figure 1L), and is absent from mature muscle fibers (Ruiz-Gomez and Bate, 1997). The characteristic pattern of Kr expression remains the same in *sltr* mutant embryos, except that each Kr-positive "cluster" is mononucleated at stage 13 (Figure 1K) but contains one to three nuclei at stage 14 (Figure 1M). These results suggest that the fate of Kr-positive founder cells is properly specified at stage 13, although these cells complete the first phase of fusion to form bi- or trinucleated syncytia at a later stage compared to wild-type. Similar results were obtained with Eve-positive founder cells. While stage 14 Eve-positive dorsal acute muscle 1 (DA1) contains approximately ten nuclei in each cluster (Figure 1F), its counterpart in *sltr* mutant embryos is mostly binucleated (Figure 1G). We conclude that *sltr* is required for the second phase of fusion to form multinucleated syncytia.

Due to its low resolution, direct visualization of myoblasts with MHC antibody (Figures 1B–1E) cannot unambiguously exclude the possibility that small fusion pores might have formed between the founder cells and the surrounding fusion-competent cells in *sltr* mutant embryos. We devised a green fluorescent protein (GFP) diffusion assay to directly test this possibility. When GFP was expressed in *sltr* mutant embryos via the founder cell-specific *rP298-GAL4* driver, we found that the GFP signal was completely retained within the Kr-positive founder cells (Figures 1N–1N″). Given the small size of GFP (a β-barrel structure with a diameter of 3.2 nm and a length

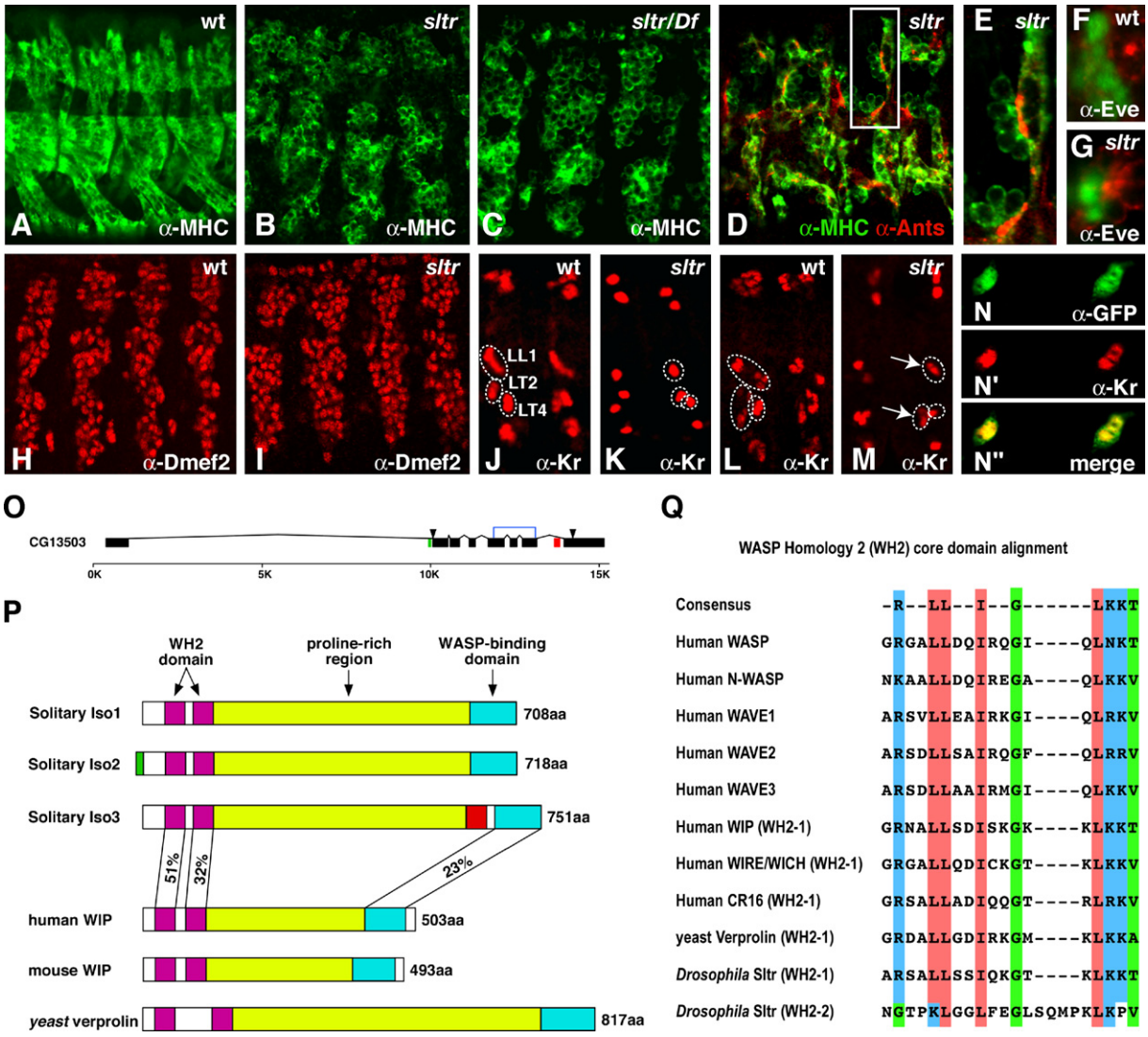

Figure 1. Genetic and Molecular Characterization of *sltr*

(A–C) Wild-type ([A]; stage 14), $sltr^{S1946}$ ([B]; stage 13), and $sltr^{S1946}$/*Df(2R)X58-7* ([C]; stage 13) embryos stained for myosin heavy chain (MHC; green). Note the presence of numerous mononucleated myoblasts in *sltr* mutants (compare [B] and [C] with [A]).

(D and E) Stage 14 *sltr* embryos stained for MHC (green) and Ants (red). (E) shows the boxed area in (D). Note that mononucleated fusion-competent cells extend filopodia and attach to elongated muscle precursors at sites where Ants is accumulated.

(F and G) Stage 14 embryos stained for Eve (green) and Titin (red). The Eve-positive DA1 cluster has an average of 9.9 ± 0.1 (n = 35) and 1.78 ± 0.1 (n = 39) nuclei in wild-type (F) and *sltr* (G) embryos, respectively.

(H and I) Stage 13 embryos stained for Dmef2 showing a similar number of Dmef2-positive nuclei in wild-type (H) and *sltr* (I) embryos.

(J and K) Stage 13 embryos stained for Kr, showing three lateral clusters (circled) containing an average of 2.6 ± 0.1 (n = 29) (LL1), 2.3 ± 0.2 (n = 28) (LT2), and 2.1 ± 0.2 (n = 27) (LT4) nuclei in wild-type (J), but single nucleus in *sltr* mutant (K).

(L and M) Stage 14 embryos showing three lateral clusters (circled) containing 3.6 ± 0.1 (n = 30) (LL1), 2.7 ± 0.1 (n = 29) (LT2), and 2.9 ± 0.2 (n = 26) (LT4) Kr-positive nuclei in wild-type (L), but mono- or binucleated clusters (arrows) in *sltr* mutant (M). The average numbers of Kr-positive nuclei in *sltr* embryos are 1.4 ± 0.1 (n = 36) (LL1), 1.5 ± 0.1 (n = 33) (LT2), and 1.4 ± 0.1 (n = 34) (LT4).

(N–N″) Complete block of fusion in *sltr* embryos. An *rP298-GAL4;* $sltr^{S1946}$/$sltr^{S1946}$, *UAS-GFP* embryo (stage 14) labeled with α-GFP (green) and α-Kr (red). Two Kr-positive precursors are shown, one of which is binucleated. Note that the GFP signal (cytoplasmic) closely matches the Kr signal (nuclear), without diffusing into adjacent fusion-competent cells.

(O) Genomic structure of the *sltr* gene. The exons encoding Sltr Iso1 are shown in black, the additional exon in Iso2 is in green, and exon 8 in Iso3 is in red. Arrowheads mark translational start and stop sites. The blue bracket indicates DNA deleted in $sltr^{S1946}$.

(P) Schematic of the isoforms of Sltr and Sltr homologs in yeast, mouse, and human. Iso1 and Iso2 are present in the embryo (see Figure S2). Amino acid identity between Sltr and its human homolog is shown.

(Q) Alignment of the WH2 core domains. Note the conservation of the Sltr WH2-1 domain, and the R → G and a K → P change in the Sltr WH2-2 domain.

of 5 nm) (Ormo et al., 1996), this result argues against the presence of any membrane openings with a diameter of $\geq$3.2 nm between the founder and the fusion-competent cells in *sltr* mutant embryos.

Molecular Characterization of *sltr*

We performed a complementation test between *sltr* and a collection of deficiencies on the second chromosome. *sltr* failed to complement *Df(2R)X58-7*, which deletes the region between 58B1-2 and 58E1-4. Transheterozygotes of *sltr* over this deficiency ($sltr^{S1946}$/*Df(2R)X58-7*) show similar phenotype as $sltr^{S1946}$ homozygous embryos (Figure 1C), with muscle DA1 in these embryos containing 1.7 ± 0.2 (n = 24) Eve-positive nuclei. Thus, $sltr^{S1946}$ behaves as a null allele. We further mapped *sltr* to 58B1-C1, as it failed to complement a smaller deficiency *Df(2R)Exel7170*, which deletes approximately 20 genes between CG10138 and CG13504. We sequenced candidate genes in this interval and found that one of them, CG13503, contained a deletion in the genomic DNA of *sltr* mutant embryos (Figure 1O). We therefore renamed CG13503 as *sltr*.

The *sltr* locus spans 15 kb and is predicted to generate six differentially spliced mRNAs (RA to RF) (BDGP; Figure 1O; Figure S2A). RT-PCR analyses revealed three differentially spliced transcripts in embryos encoding a 708 amino acid (Iso1) and a 718 amino acid (Iso2) variant (Figure 1P; Figure S2). Notably, the predicted exon 8 (E8) is absent from the embryonic transcripts. Database searches revealed that Sltr represents the sole *Drosophila* homolog of the yeast very proline-rich protein (verprolin) and human WASP-interacting protein (WIP) (Figure 1P).

Yeast verprolin and mammalian WIP are important regulators of the actin cytoskeleton (reviewed by Anton and Jones, 2006). In mammalian cells, WIP forms a stable complex with WASP, which in turn regulates actin polymerization via the Arp2/3 complex. The importance of the WIP-WASP interaction is highlighted by the fact that the majority of Wiskott-Aldrich patients carry missense mutations in the WH1 domain of WASP, a domain which is required for WIP binding (Volkman et al., 2002). Despite its broad expression (Ramesh et al., 1997), WIP-deficient mice appear largely normal, with the exception of defective T cell activation due to subcortical actin-filament defects (Anton et al., 2002). The subtlety of the WIP knockout phenotype could be partly explained by the existence of additional WIP-related proteins in mammals such as WIRE/WICH and CR16 (reviewed by Anton and Jones, 2006). The presence of a single WIP-like protein in *Drosophila* should overcome the difficulties in studying potentially redundant WIPs in mammals.

Sltr contains two WASP homology 2 (WH2) domains, a proline-rich region and a WASP-binding domain (WBD) (Ramesh et al., 1997; Paunola et al., 2002). The WH2 domain has been shown to bind to monomeric actin through an amphiphilic α helix and an LKKT motif (Chereau et al., 2005). While the core region of the first WH2 domain in Sltr (amino acids 34–51) contains all the critical residues required for actin binding, that of the second WH2 domain (amino acids 101–122) has a K → P change in the highly conserved LK*K*T motif as well as an R → G change in the amphiphilic α helix (Figure 1Q). These amino acid substitutions abolish the binding of the second WH2 domain to G-actin (see below). The $sltr^{S1946}$ allele deletes 1.2 kb genomic DNA spanning three exons that encode part of the proline-rich region (Figure 1O), resulting in a truncated protein of 325 amino acids (numbering according to Iso1).

Sltr Is Specifically Expressed in Fusion-Competent Myoblasts

As a starting point to characterize Sltr function, we examined the expression of *sltr* mRNA in *Drosophila* embryos. In contrast to the widespread expression of WIP in mammals, *sltr* is expressed specifically in the developing musculature (Figures 2A–2C). *sltr* mRNA is first detected in the visceral and somatic muscles at stage 11 when myoblast fusion is initiated (Figure 2A), persists in the somatic muscle cells until the end of stage 14 when fusion is completed (Figures 2B and 2C), and disappears from the mature muscle fibers thereafter (data not shown). Antibody staining showed that the Sltr protein is expressed in a similar pattern (Figures 2D–2F).

In order to determine in which myoblast population Sltr is expressed, we compared the localization of Sltr with that of Ants, which marks the cytoplasm of founder cells, and Dmef2, which marks the nuclei of both founder and fusion-competent cells. As shown in Figure 2G, Sltr is detected in the cytoplasm surrounding the nuclei of fusion-competent cells. The expression of Sltr and Ants appears to be exclusive of each other, suggesting that Sltr might be specifically present in fusion-competent cells. To test this possibility further, we marked the founder cell membrane using *rP298-GAL4; UAS-CD8GFP* and examined the relative expression of GFP and Sltr. As shown in Figure 2H, Sltr expression is excluded from the GFP-labeled founder cells, suggesting that Sltr is exclusively expressed in fusion-competent cells. Definitive proof for this conclusion was obtained by examining the expression of Sltr in *lmd* mutant embryos, which lack all fusion-competent cells. As shown in Figures 2J and 2J‴, Sltr expression is absent in the somatic musculature in the *lmd* mutant embryo. Thus, we conclude that Sltr is specifically expressed in fusion-competent cells. We noticed that Sltr is present in multinucleated myotubes in late-stage embryos (Figures 2I and 2I′), presumably due to diffusion of the Sltr protein from fusion-competent cells to fused myotubes.

Sltr Is Localized to Sites of Fusion

Careful examination revealed a nonuniform subcellular localization of the Sltr protein in the cytoplasm of fusion-competent cells. Notably, specific foci with strong Sltr expression are detected (Figures 2K and 2L). These foci are reminiscent of those reported for other proteins required for fusion. Indeed, the Sltr-positive foci colocalize with the fusion receptor, Sns, and the structural protein, Titin, both of which are known to aggregate to sites of fusion (Figures 2K–2K‴). Furthermore, the localization of Sltr to

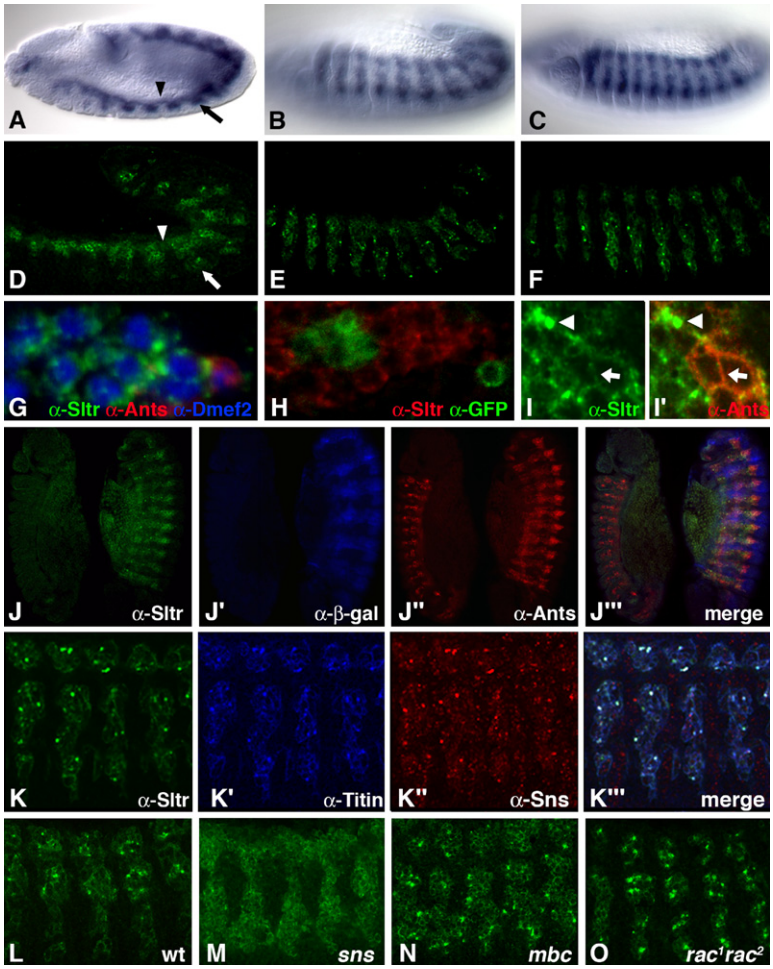

Figure 2. Expression and Subcellular Localization of the Sltr Protein at Sites of Fusion in Fusion-Competent Cells

(A–C) *sltr* mRNA expression revealed by in situ hybridization.

(D–F) Sltr protein expression stained by α-Sltr antibody.

(G) A wild-type stage 13 embryo labeled with α-Sltr (green), α-Ants (red), and α-Dmef2 (blue). Note the close association of the Sltr signal with fusion-competent cells (blue nuclei), but not with the founder cell (red).

(H) A stage 13 *rP298-GAL4; UAS-CD8GFP* embryo double labeled with α-Sltr (red) and α-GFP (green). Note the mutual exclusion of the Sltr signal with that of the founder cell-specific GFP signal.

(I and I′) A stage 14 embryo showing the presence of Sltr (green) in fused myotubes marked by α-Ants (red) (arrow). Note that there is still high-level Sltr in discrete foci (arrowhead).

(J–J‴) Stage 13 embryos produced by *lmd/TM3, ftz-lacZ* parents were labeled with α-Sltr (green), α-β-gal (blue), and α-Ants (red). The control (right) and mutant (left) *lmd* embryos can be unambiguously identified based on the absence of β-gal signal in the homozygous *lmd* embryo. Note that Ants, but not Sltr, is present in the *lmd* mutant embryo.

(K–K‴) Localization of Sltr to sites of fusion. A wild-type embryo labeled with α-Sltr (green), α-Titin (blue), and α-Sns (red). Note the colocalization of the Sltr-positive foci with those of Titin and Sns (appearing as white spots in the merged image).

(L–O) Wild-type (L), *sns* (M), *mbc* (N), and rac^1rac^2 (O) embryos labeled by α-Sltr. Sltr-positive foci are present in wild-type, *mbc*, and rac^1rac^2 embryos, but absent in *sns* embryos.

sites of fusion is dependent on the fusion receptor Sns, as Sltr protein is evenly distributed in the cytoplasm of fusion-competent cells in *sns* mutant embryos (Figure 2M). This change in Sltr subcellular localization is not simply due to lack of fusion, as Sltr-positive foci are still present in other fusion mutants such as *mbc* or rac^1rac^2 (Figures 2N and 2O). These results also indicate that the recruitment of Sltr to the fusion receptor Sns is independent of the Mbc → Rac → WAVE pathway.

Sltr Is an Actin- and WASP-Binding Protein

The presence of WH2 and WBD domains in Sltr suggests that Sltr may interact with G-actin and WASP. A GST fusion protein containing an N-terminal fragment of Sltr with two WH2 domains (N) was found to bind monomeric G-actin (Figures 3A and 3B). Interestingly, a point mutation of a conserved lysine within the first WH2 domain (N-K49Q), a deletion of the first WH2 domain (N-ΔWH2-1), or deletion of both WH2 domains (N-ΔWH2-1&2), all abolished the G-actin-binding activity, whereas deleting the second WH2 domain (N-ΔWH2-2) did not affect this activity (Figure 3B). Thus, the first, but not the second, WH2 domain of Sltr binds to G-actin. These results are consistent with the high degree of conservation of the first, but not the second, WH2 domain of Sltr (Figure 1Q).

Previous studies have shown that the mammalian homologs of Sltr (WIP, WICH/WIRE, and CR16) associate with F-actin as well as G-actin (reviewed by Anton and Jones, 2006). We therefore tested whether Sltr binds to F-actin by cosedimentation assays. As shown in Figure 3C, the N-terminal fragment of Sltr (N) binds to F-actin, which is consistent with previous studies mapping the F-actin-binding site to the N-terminal region of human WIP (Martinez-Quiles et al., 2001). We further tested which sequence(s) within N binds F-actin. Interestingly, deleting the first WH2 domain (N-ΔWH2-1) did not affect F-actin binding, whereas deleting the second WH2 domain (N-ΔWH2-2) impaired the ability of N to bind F-actin (Figure 1C). These results demonstrate that while G-actin binds to the first WH2 domain, F-actin interacts preferentially with the second WH2 domain and its flanking sequences. Thus, G-actin and F-actin bind to different regions in Sltr.

We performed coimmunoprecipitation (co-IP) assays to detect potential interactions between Sltr and WASP. As shown in Figure 3D, a Flag-tagged Sltr coprecipitated

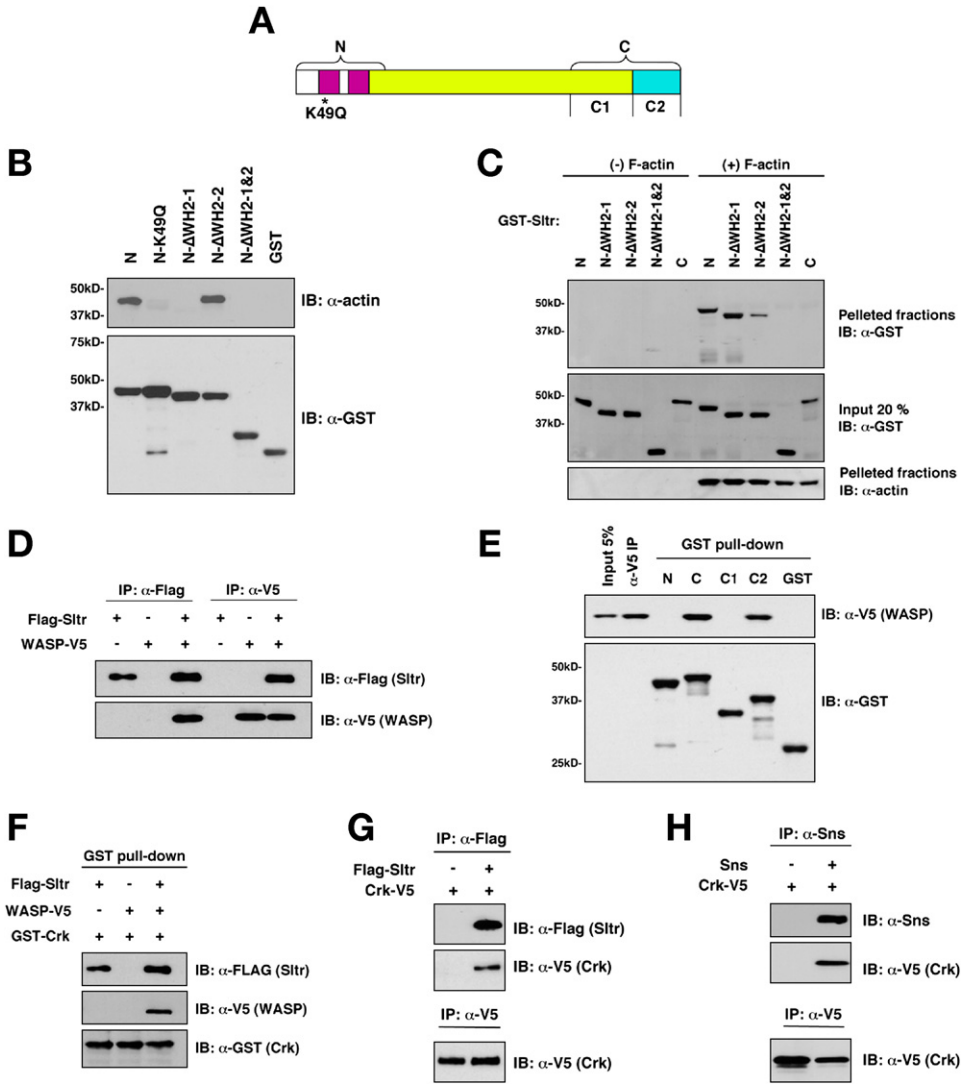

Figure 3. Sltr Interacts with Actin, WASP, and Crk

(A) Schematic diagram of Sltr, as well as the point mutation and N- and C-terminal fragments used in these binding assays.

(B) GST pull-down assay showing that the first (WH2-1), but not the second (WH2-2), WH2 domain of Sltr binds G-actin.

(C) F-actin cosedimentation assay showing that WH2-2 is involved in F-actin binding.

(D) Extracts from S2R+ cell transfected with the indicated plasmids were immunoprecipitated (IP) and probed (IB) with the indicated antibodies, showing specific association between Sltr and WASP.

(E) WASP-V5 expressed in S2R+ cells was incubated with the indicated GST fusion proteins in a GST pull-down assay.

(F) GST-Crk was incubated with S2R+ extracts expressing the indicated epitope-tagged proteins. Note that GST-Crk can pull down WASP-V5 only in the presence of Flag-Sltr.

(G) Co-IP of Crk-V5 with Flag-Sltr expressed in S2R+ cells.

(H) Co-IP of Crk-V5 with Sns expressed in S2R+ cells.

with a V5-tagged WASP expressed in *Drosophila* S2R+ cells. GST pull-down assays were carried out to map the WASP-binding domain within Sltr. A C-terminal fragment encompassing the predicted WBD, but not the N-terminal region, efficiently pulled down the V5-tagged WASP (Figure 3E). Further mapping of the C-terminal region revealed that a smaller fragment containing merely the WBD (C2), but not a fragment without the WBD (C1), pulled down WASP-V5 (Figure 3E), demonstrating that Sltr interacts with WASP through its WBD domain.

The Small Adaptor Protein Crk Provides a Potential Link between Sltr and the Fusion Receptor Sns

The presence of a proline-rich region suggests that Sltr may interact with SH3 domain-containing proteins. A relevant candidate in myoblast fusion is the SH2 and SH3 domain-containing adaptor protein Crk. While a loss-of-function mutant for *Drosophila* Crk is not available, overexpression of a membrane-targeted form of Crk is known to cause a myoblast fusion defect (Abmayr et al., 2003). GST pull-down and co-IP assays were performed to test

potential interactions between Sltr and Crk. As shown in Figure 3F, GST-Crk was able to pull down Flag-tagged Sltr expressed in S2R+ cells. In addition, V5-tagged Crk coimmunoprecipitated with Flag-tagged Sltr in S2R+ cells (Figure 3G), further supporting a physical association between these two proteins.

It is formally possible that the interaction between Sltr and Crk is mediated by WASP, as WASP also contains a proline-rich domain (reviewed by Miki and Takenawa, 2003) and it forms a tight complex with Sltr (this study). However, GST-Crk could not pull down WASP-V5 expressed alone in S2R+ cells (Figure 3F), arguing against a direct interaction between Crk and WASP. Interestingly, GST-Crk effectively pulled down WASP-V5 when Flag-Sltr was coexpressed, consistent with the idea that Sltr mediates the formation of the Crk-Sltr-WASP complex.

Because SH2 and SH3 domain-containing proteins are known to mediate interactions between membrane receptors and downstream effectors, we tested whether Crk may interact with the fusion-competent cell receptor Sns. As shown in Figure 3H, a co-IP assay revealed a specific interaction between Sns and V5-tagged Crk in S2R+ cells. Taken together, these results suggest that Crk may be the adaptor protein that recruits Sltr to sites of fusion defined by Sns in vivo.

Sltr Induces Actin Polymerization by Interacting with Actin and WASP

Studies of mammalian WIP have thus far provided conflicting evidence on WIP's function in actin polymerization. While biochemical analysis suggested an inhibitory role for WIP in actin polymerization (Martinez-Quiles et al., 2001), cell culture studies showed that WIP promotes the formation of actin-rich filopodia (Martinez-Quiles et al., 2001; Ramesh et al., 1997). We took advantage of *Drosophila* S2 cells to investigate Sltr's role in actin polymerization. Overexpressing Sltr in S2 cells resulted in a dramatic increase in F-actin, leading to the formation of numerous actin-filled microspikes, a phenotype observed in 100% of the transfected cells (compare Figures 4Aa–4Aa″ and Figures 4Ab–4Ab″). Deletion of the first WH2 domain (SltrΔWH2-1) or a point mutation of a conserved lysine in WH2-1 (SltrK49Q) significantly reduced F-actin-inducing activity, suggesting that G-actin binding is required for Sltr to promote actin polymerization (Figures 4Ac–4Ad″). Interestingly, deleting the second WH2 domain (SltrΔWH2-2) also reduced the number of microspikes but to a less extent compared to SltrΔWH2-1 (Figures 4Ae–4Ae″). Not surprisingly, when both WH2 domains are deleted, microspike formation was abolished (Figures 4Af–4Af″). The F-actin-inducing activity of Sltr also requires WASP, as deletion of the WBD (SltrΔWBD), or a knockdown of endogenous WASP through RNAi, abolished this activity (Figures 4Ag–4Ah″). Taken together, we conclude that Sltr positively regulates actin polymerization by interacting with G-actin, F-actin, and WASP.

The functional importance of the WH2 and WBD domains was further tested by in vivo rescue assays. Full-length Sltr rescued the myoblast fusion defect in *sltr* mutant embryos (Figures 4Bi and 4Bj). However, mutations that remove one or both WH2 domains, that change a critical residue (K49Q) in the first WH2 domain, or that delete the WBD, all failed to rescue the fusion phenotype, despite the proper localization of mutant proteins to cell contact sites (Figures 4Bk–4Bo; Figure S3). Thus, the same domains that affect actin polymerization are equally important for myoblast fusion in vivo.

WASP Is Required for Myoblast Fusion

The importance of the WBD for Sltr's function in myoblast fusion suggests that WASP may also be required for this process. *Drosophila* has a single WASP homolog, *Wasp*, which has been shown to function in asymmetric cell division during embryogenesis (Ben-Yaacov et al., 2001). However, its potential function in muscle development has not been reported. To examine Wasp's function during myogenesis, we generated germline clones of *Wasp* (*Wasp*$^{mat/zyg}$) which eliminate both maternal and zygotic expression of the gene. As shown in Figure 4Bp, *Wasp*$^{mat/zyg}$ embryos exhibit a severe loss-of-fusion phenotype, similar to that of *sltr* mutant embryos, further supporting our model that Sltr functions through WASP to regulate myoblast fusion.

Sltr Is Required for Localized Induction of Actin Polymerization at Sites of Fusion

The effect of Sltr on actin polymerization in S2 cells and the requirement of its WH2 and WBD domains in vivo strongly indicate a role for Sltr in regulating actin polymerization during myoblast fusion. To investigate this possibility, we visualized F-actin in stage 13 embryos by phalloidin staining. Interestingly, F-actin-rich foci are observed colocalizing with those of Sltr and Titin at sites of fusion (Figures 5A–5A″ and 5B–5B″). Like Sltr, formation of the F-actin foci requires the fusion receptor Sns, as they are absent in *sns* mutant embryos (Figures 5C–5C″). Careful analyses of pairs of adjacent founder/myotube and fusion-competent cells revealed that F-actin is enriched at cell contact sites between these two types of cells and that a larger portion of a given F-actin focus colocalizes with Sltr residing in fusion-competent cells, whereas a smaller portion of the same focus colocalizes with Ants in founder cells (Figures 5D–5F‴). Given the function of Sltr in promoting actin polymerization in cultured cells, colocalization between Sltr and F-actin indicates that Sltr may be involved in inducing actin polymerization at sites of fusion. Indeed, F-actin foci are greatly diminished in fusion-competent cells in *sltr* mutant embryos, whereas F-actin gradually accumulates to an abnormally high level in the adjacent founder cell along the apposing membranes (Figures 5G–5I‴). Taken together, Sltr is required for receptor-triggered induction of actin polymerization at sites of fusion in fusion-competent cells.

Sltr Is Required for Targeted Exocytosis of Prefusion Vesicles to the Plasma Membrane

The presence of F-actin foci at sites of fusion and their aberrant behavior in *sltr* mutants strongly suggest that actin

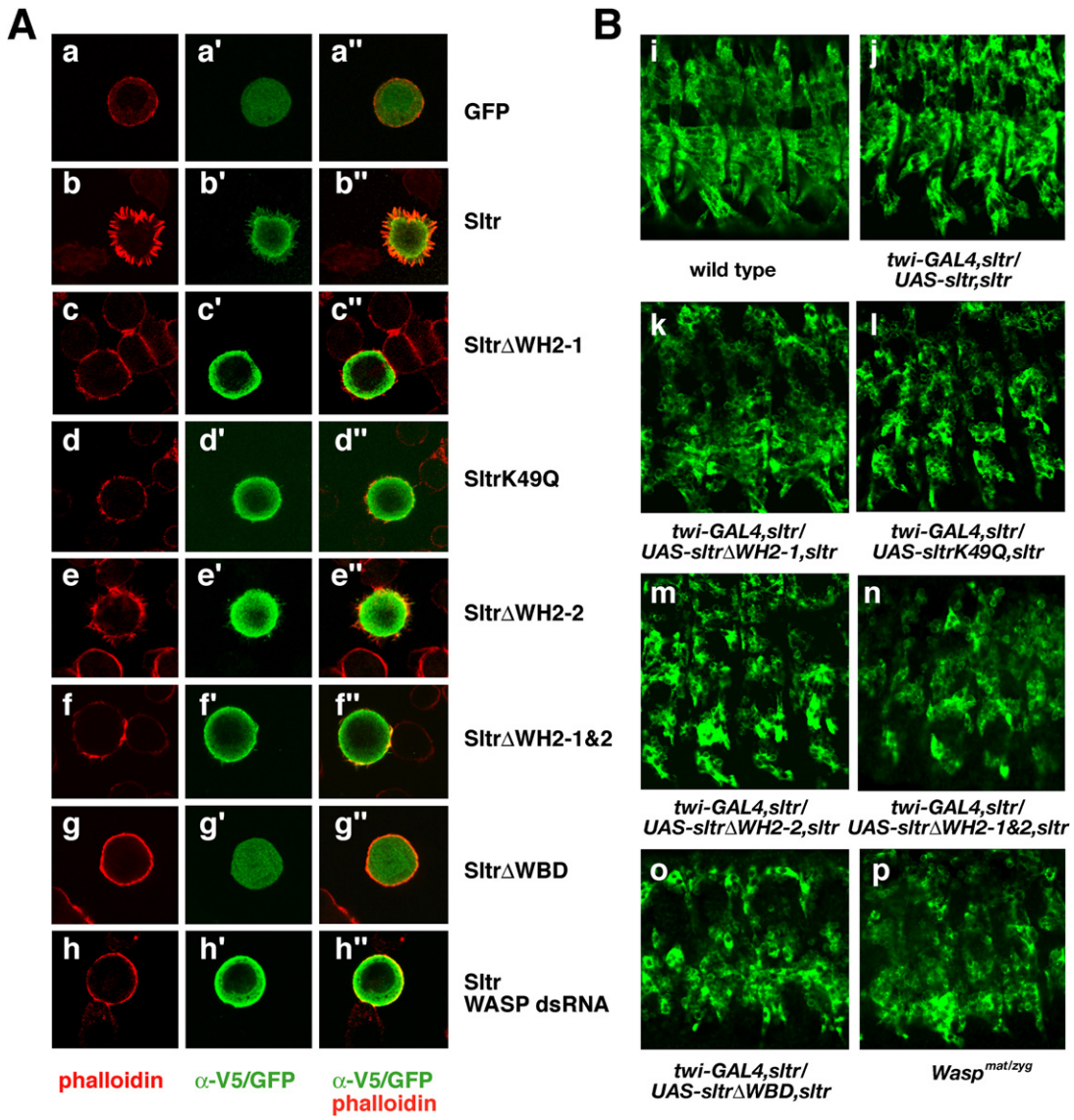

Figure 4. Sltr Promotes Actin Polymerization and the Requirement of WH2 and WBD Domains for Sltr Function In Vivo

(A) S2 cells expressing V5-tagged wild-type and the indicated mutant Sltr proteins or dsRNA were stained for F-actin (phalloidin, red) and α-V5 (green). (B) (i–o) Wild-type and *sltr* embryos expressing the indicated transgenes were labeled by α-MHC. The fusion defect was rescued by the wild-type transgene (j), but not any of the mutant transgenes (k–o). (p) The lack-of-fusion defect of a *Wasp* germline clone (*Wasp*$^{mat/zyg}$) embryo.

cytoskeleton rearrangement plays an important role during myoblast fusion. To investigate the precise function of the actin cytoskeleton during fusion, we performed electron microscopy (EM) analysis. We focused on the ventral group of muscles, which have been best characterized by EM (Doberstein et al., 1997). In wild-type embryos, paired vesicles (~40 nm in diameter) with electron-dense margins form at the contact sites between founder and fusion-competent cells (Doberstein et al., 1997; Figures 6A–6A″). However, the origin and function of these vesicles are not known. In wild-type myoblasts, we observed electron-dense vesicles (~40 nm in diameter) in the vicinity of the Golgi, as well as in the process of budding off from the Golgi (Figures 6E–6E″), indicating that these vesicles are of exocytic origin. We also observed a frequent association of these vesicles with microtubules (Figures 6F–6F″), suggesting that they are transported to the cell periphery via the microtubule network.

In *sltr* mutant myoblasts, while we also observed a close association between the vesicles and the microtubule network (Figures S4A–S4B′), these vesicles have a profound defect in membrane targeting. Specifically, paired vesicles are found not only at sites of fusion between the apposing founder and fusion-competent cells but also between neighboring fusion-competent cells (Figures 6C–6C″). The absence of actin-rich foci (Figures 5G–5I‴) and the ectopic routing of vesicles to the plasma

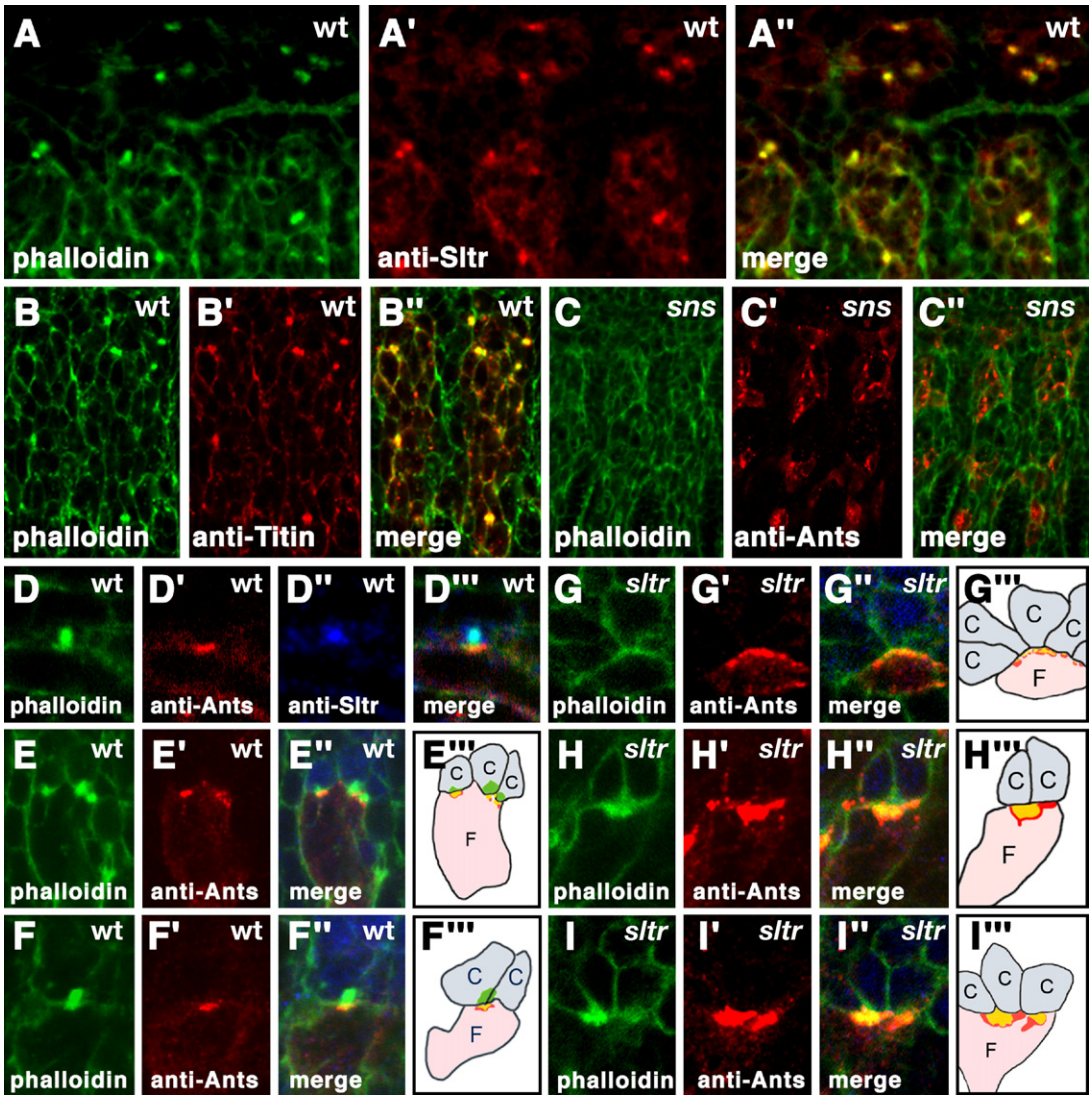

Figure 5. Sltr Colocalizes with F-Actin Foci and Is Required for Localized Actin Polymerization at Sites of Fusion in Fusion-Competent Cells

In all panels, F-actin is labeled by FITC-conjugated phalloidin (green).

(A–A″) Sltr (red) colocalizes with F-actin foci in a wild-type embryo.

(B–B″) F-actin foci colocalize with Titin (red) in a wild-type embryo.

(C–C″) Absence of F-actin foci in an *sns* mutant embryo. Note the presence of Ants foci (red) in the founder cells.

(D–D‴) An F-actin focus at a cell contact site between fusing myoblasts. Sltr (blue) colocalizes with a larger portion of the actin focus in the fusion-competent cell, whereas Ants (red) colocalizes with a smaller portion of the actin focus in the founder cell.

(E–I‴) F-actin at cell contact sites in wild-type (E–F‴) and *sltr* mutant (G–I‴) embryos. Founder cells are labeled by α-Ants (red) and fusion-competent cells by α-Lmd (blue). In the schematics (E‴, F‴, G‴, H‴, and I‴), F stands for founder cell and C stands for fusion-competent cell.

(E–F‴) Two examples of F-actin foci at sites of fusion between founder and fusion-competent cells in stage 13 wild-type embryos. Note that F-actin is enriched on both sides of the apposed membranes, although the F-actin foci appear to be larger in fusion-competent cells.

(G–G″) F-actin distribution in a stage 13 *sltr* mutant embryo. Note that the amount of F-actin is greatly diminished in the fusion-competent cells and starts to accumulate in the founder cell.

(H–I‴) Two examples of F-actin phenotype in stage 14 *sltr* mutant embryos. F-actin is nearly absent from fusion-competent cells, but accumulates as elongated patches in the founder cells along the cell-cell contact sites.

membrane in *sltr* mutant fusion-competent cells suggest that localized actin polymerization at sites of fusion may normally provide a positional cue for vesicle transport. To further corroborate this model, we visualized the spatial relationship between the actin-rich foci and exocytic vesicles in myoblasts using immuno-EM. This analysis revealed a high concentration of actin adjacent to myoblast contact sites (Figures 6G and 6G′; Figures S4C–S4D′), which likely correspond to the actin-rich foci observed using fluorescent microscopy (Figure 5). Two different

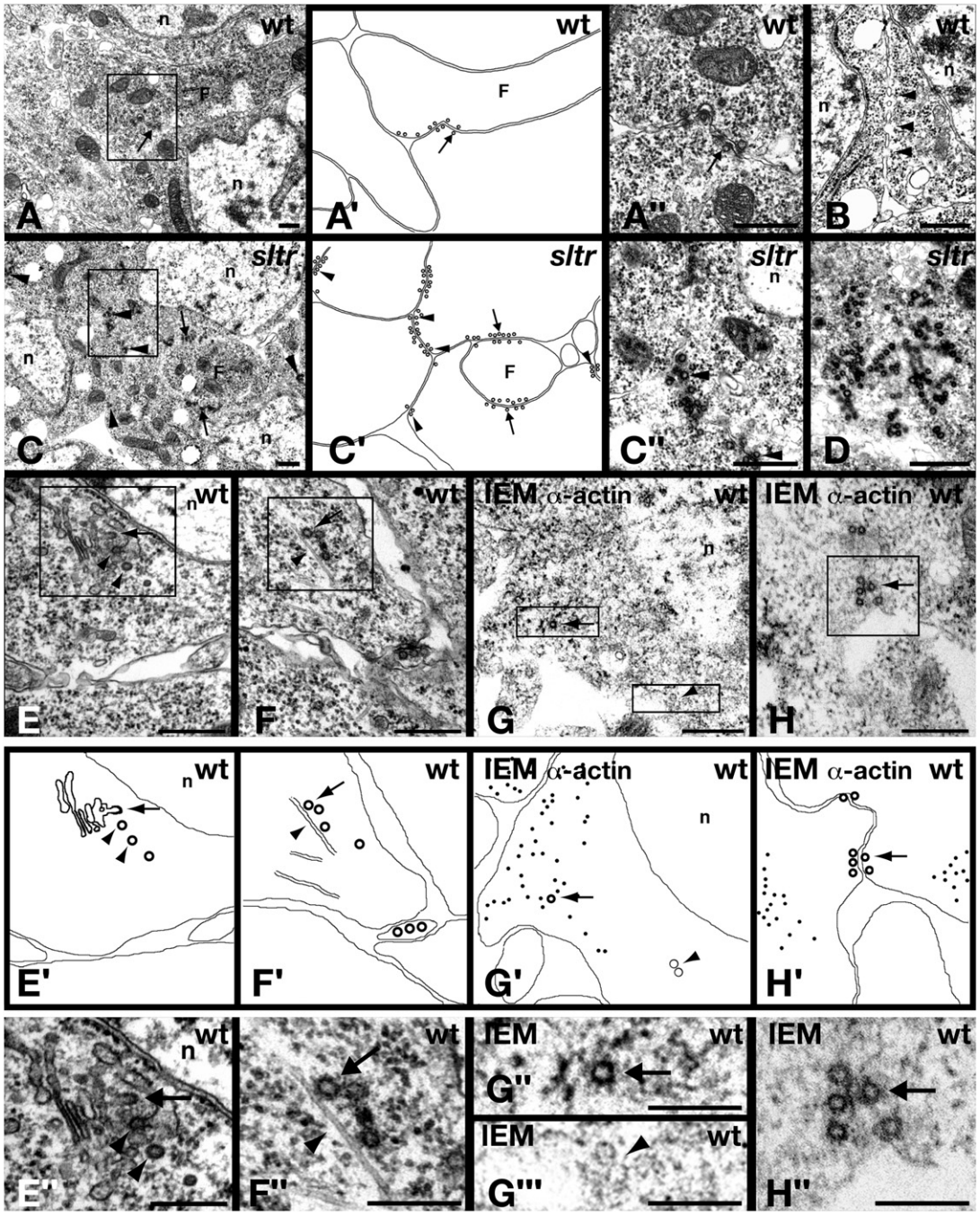

Figure 6. Sltr and Actin-Rich Foci Are Involved in Vesicle Targeting and Coating

Conventional electron microscopy (A–F″) and immuno-EM (G–H″) micrographs of wild-type and *sltr* mutant embryos. Schematic drawings for (A), (C), (E), (F), (G), and (H) are shown in (A′), (C′), (E′), (F′), (G′), and (H′), respectively. Boxed areas in (A), (C), (E), (F), (G), and (H) are enlarged in (A″), (C″), (E″), (F″), (G″/G‴), and (H″), respectively.

(A–A″) Vesicles (~40 nm diameter) with an electron-dense margin are present between founder and fusion-competent cells at early stage 13 in a wild-type embryo. The founder cell, labeled F, is inferred by its relative position in a cluster of myoblasts. The arrow points to vesicles with electron-dense margins; n, myoblast nuclei.

(B) Fusion pores (arrowheads) in a stage 13 wild-type embryo.

(C–C″) In an early stage 14 *sltr* mutant embryo, prefusion vesicles are present not only between founder and fusion-competent cells (arrows) but also along the membranes of adjacent fusion-competent cells (arrowheads).

(D) Accumulation of prefusion vesicles in a stage 14 *sltr* mutant embryo.

(E–F″) Intracellular localization of prefusion vesicles in early stage 13 embryos.

(E–E″) Prefusion vesicles are observed budding off from the Golgi (arrow), or in the vicinity of the Golgi (arrowhead).

classes of vesicles are also evident (Figures 6G″, 6G‴, and 6H″). The first class of vesicles are "actin coated," which are present either within the actin-rich patches or as paired vesicles aligned at the plasma membrane (Figures 6G″ and 6H″; Figures S4C–S4D′). The second class of vesicles, which reside outside of the actin foci, are devoid of α-actin staining (Figure 6G‴). We infer that the former class of vesicles acquires actin coating when they transit through the actin foci en route to the plasma membrane. Interestingly, actin-rich patches are observed at the cell cortex only in "immature" myoblasts containing vesicles in their cytoplasm (Figures 6G and 6G′; Figures S4C–S4D′), but not in "mature" myoblasts in which vesicles have already paired along the plasma membrane, suggesting that these actin-rich patches are transient structures that disintegrate once vesicles have reached the plasma membrane.

Besides the mistargeting phenotype, the exocytic vesicles also persist much longer in *sltr* mutant myoblasts. In wild-type embryos, once vesicles reach sites of fusion, they rapidly resolve into electron-dense plaques followed by the formation of fusion pores between the aligned membranes (Doberstein et al., 1997; Figure 6B). As a result, fusion of wild-type myoblasts occurs quickly and is completed in the ventral group of muscles at stage 13 (Doberstein et al., 1997). In *sltr* mutant embryos, although vesicles start to appear by the end of stage 13 as in the wild-type, they never resolve. Instead, the vesicles are still present in stage 14 *sltr* embryos, long after the wild-type myoblasts have completed fusion (Figures 6C and 6C′), and further accumulate to large numbers in late stage 14 embryos (Figure 6D). These vesicles eventually disappear from the mutant myoblasts (data not shown). The prolonged accumulation of vesicles suggests that besides mistargeting, these vesicles might also be defective in fusing to the plasma membrane in *sltr* mutant myoblasts.

To further investigate whether the fusion process is completely blocked at the vesicle-plasma membrane fusion stage or whether it could proceed beyond this point in *sltr* mutant embryos, we looked for the presence, or absence, of electron-dense plaques and membrane discontinuities (fusion pores) along the apposing membranes between founder and fusion-competent cells. No electron-dense plaques were observed in *sltr* mutant embryos, though such plaques are rarely seen in wild-type embryos as well (Doberstein et al., 1997). To our surprise, membrane discontinuities (≥40 nm in diameter) were observed in *sltr* mutant embryos prepared by the conventional chemical fixation method (data not shown). This result does not agree with that of the GFP diffusion assay (Figures 1N–1N″), which indicates the absence of any membrane openings ≥3.2 nm in diameter between the founder and the fusion-competent cells. Because conventional EM using chemical fixation is known to generate "fixation artifacts" due to slow diffusion of fixatives into cells, we used the high-pressure freezing (HPF) method (McDonald and Auer, 2006), which allows better preservation of cells with ultrarapid freezing of cellular structures, to visualize the plasma membrane between apposing myoblasts. As shown in Figure S5, and in agreement with the GFP diffusion assay, the cell membrane between founder and fusion-competent cells remains completely intact in late stage 14 *sltr* embryos prepared using the HPF method. We conclude that myoblast fusion is blocked prior to the vesicle-plasma membrane fusion stage in *sltr* mutant embryos.

WIP and WASP Are Required for Myoblast Fusion in Mouse C2C12 Cells

The requirement of Sltr and WASP for myoblast fusion in *Drosophila* prompted us to ask whether their mammalian counterparts are involved in a similar process. In mammals, there are two WASP proteins (WASP and N-WASP) and three WIP homologs (WIP, WIRE/WICH, and CR16). While WASP and CR16 are mainly expressed in the hematopoietic system and the brain, respectively, N-WASP, WIP, and WIRE are widely expressed (reviewed by Anton and Jones, 2006; Miki and Takenawa, 2003). Previous studies in mouse myoblast culture C2C12 cells revealed a function of N-WASP in myoblast migration (Kawamura et al., 2004). However, its potential function in myoblast fusion has not been reported. We explored this possibility by RNA interference experiments. As shown in Figure 7A, N-WASP, WIP, and WIRE are all expressed in C2C12 cells. RNAi knockdown of WIP or N-WASP, but not WIRE, significantly reduced fusion between myoblasts (Figures 7Ba–7Bd and 7C). These results suggest that WIP and N-WASP are important for myoblast fusion, though it is not clear at present which specific step(s) of the fusion process WIP and N-WASP are involved in. An actin-filament destabilizing agent, latrunculin A, also inhibited the fusion of C2C12 cells (Figures 7Be and 7C), consistent with an involvement of the actin cytoskeleton in C2C12 myoblast fusion.

(F–F″) Prefusion vesicles (arrow) are associated with microtubules (arrowhead).
(G–H″) Immuno-EM with α-actin antibody. Compared to conventional EM (A–F″), no lead staining was performed for immuno-EM. As a result, most of the intracellular electron-dense structures revealed by conventional EM, including the Golgi, microtubules, and ribosomes, appear either very faint or are not detectable by immuno-EM. The dark grains in the immuno-EM panels represent silver-enhanced gold particles conjugated to the secondary antibody.
(G) An actin-positive patch is observed adjacent to the plasma membrane of a myoblast. A prefusion vesicle residing in the actin patch is coated with gold particles (arrow; close-up view in [G″]). Note that even though the vesicle may look similar to the electron-dense vesicles visualized by conventional EM, it is visualized differently such that its dark margin is due to α-actin staining instead of lead staining. Two vesicles outside of the actin patch appear very faint without α-actin or lead staining (arrowhead; close-up view in [G‴]).
(H) Vesicles that have reached the apposing membranes remain coated with actin. Note that the actin-positive patch adjacent to the plasma membrane is nearly absent, with only a small amount of residual actin farther away from the membrane (dark grains) in (H) and (H′).
The scale bars represent 500 nm in all panels except for (E″), (F″), (G″), (G‴), and (H″), where they represent 250 nm.

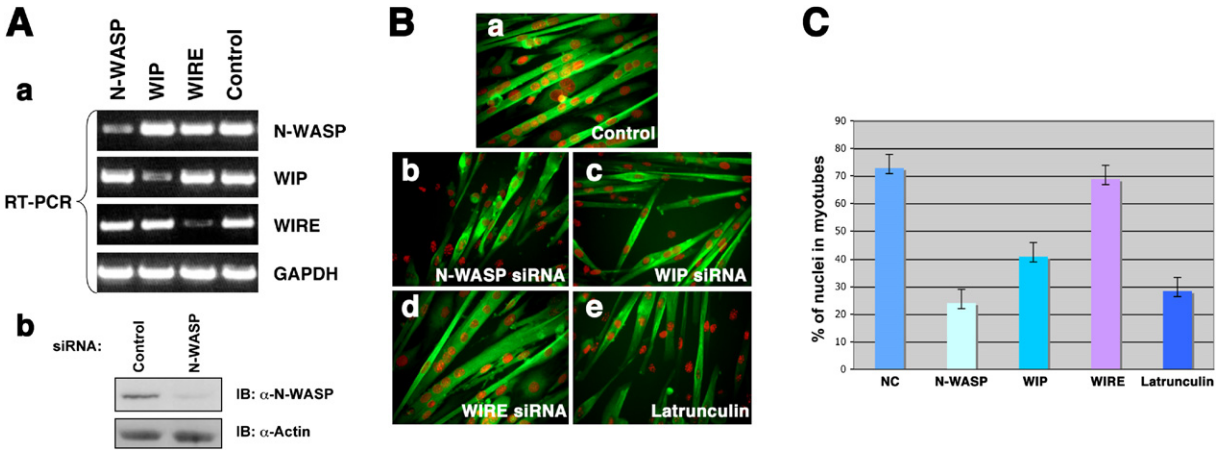

Figure 7. Mouse WIP and WASP Are Involved in Myoblast Fusion

(A) Knockdown of N-WASP, WIP, and WIRE by siRNA in C2C12 cells monitored by RT-PCR (a) and western blot (b).

(B) siRNA-transfected or latrunculin A-treated C2C12 cells were allowed to differentiate and were stained with Hoechst 33342 (red) and α-MHC (green) to visualize nuclei and differentiated myoblasts/myotubes, respectively. Note that knockdown of N-WASP (b) or WIP (c), or latrunculin A treatment (e), partially blocks myoblast fusion (compared to [a]). Knockdown of WIRE has no effect (d).

(C) Quantitation of experiments in (B). The fusion index is calculated as the percentage of nuclei in fused myotubes out of the total number of nuclei for each 20× field. Cells with ≥2 nuclei were counted as a fused myotube. Each bar represents the mean ± standard error of thirty 20× fields from three independent experiments.

DISCUSSION

Our characterization of Sltr provides a number of novel, and somewhat unexpected, findings concerning the role of the actin cytoskeleton in myoblast fusion. In contrast to the widespread expression of WIP in mammals, Sltr is specifically expressed in developing muscles and, moreover, only in fusion-competent myoblasts. Such cell-type specificity is unexpected, given that Sltr is the only WIP homolog in *Drosophila*. As a positive regulator of actin polymerization, Sltr is recruited to sites of fusion by the fusion receptor Sns and is required for the formation of F-actin-enriched foci at these sites. Our EM studies suggest that these actin-rich foci may provide directionality for the trafficking of prefusion vesicles, which are routed to ectopic membrane sites in the fusion-competent cells in *sltr* mutant embryos. We suggest that targeted exocytosis of prefusion vesicles represents a critical step leading to plasma membrane fusion.

Sltr Mediates Signaling from the Fusion Receptor to the Actin Cytoskeleton in Fusion-Competent Cells

The identification of Ants/Rols7 as a founder cell-specific protein that mediates signaling from the fusion receptor Duf to the actin cytoskeleton (Chen and Olson, 2001; Menon and Chia, 2001; Rau et al., 2001) suggests the existence of a fusion-competent cell-specific protein(s) with an analogous function. Our current work suggests that Sltr represents such a molecule. Not only is Sltr recruited to sites of fusion by the fusion-competent cell-specific receptor Sns, likely mediated by the small adaptor protein Crk, it also brings the actin polymerization machinery to these sites by binding to WASP and G-actin. As a result, Sltr colocalizes with F-actin-rich foci at sites of fusion, and is required for the formation of these actin foci in fusion-competent cells. Thus, like Ants/Rols7 in founder cells, Sltr is a fusion-competent cell-specific protein that links the fusion receptor with the actin cytoskeleton (Figure 8A).

How does Sltr regulate actin polymerization? Our in vitro and in vivo assays demonstrate that this activity is mediated by the WH2 and WBD domains of Sltr, which bind to actin and WASP, respectively. In *Drosophila* S2 cells, overexpression of Sltr, but not mutant forms lacking the WH2 or WBD domains, leads to profound changes in actin cytoskeleton organization characterized by the formation of F-actin-filled microspikes. Likewise, the ability of Sltr to rescue *sltr* mutant embryos requires the WH2 and WBD domains. These observations suggest that both actin and WASP binding contribute to Sltr function. Interestingly, while the first WH2 domain of Sltr binds to G-actin, the second WH2 domain and its flanking region interact with F-actin. Thus, the actin-binding activity of Sltr serves a dual role—it not only provides a pool of monomeric G-actin (in addition to the G-actin recruited by WASP) at sites of fusion but also stabilizes the newly formed actin filaments. The importance of the WASP-binding activity in Sltr function is further supported by the observation that RNAi knockdown of WASP abolished the ability of Sltr to induce microspikes in S2 cells, and that WASP itself is required for myoblast fusion in *Drosophila*. How WASP activity is regulated in myoblast fusion remains to be determined. Although mammalian WASP is known to be activated by the small GTPase Cdc42, this is unlikely the case in *Drosophila* myoblast fusion, as expression of a dominant-negative Cdc42 does not cause

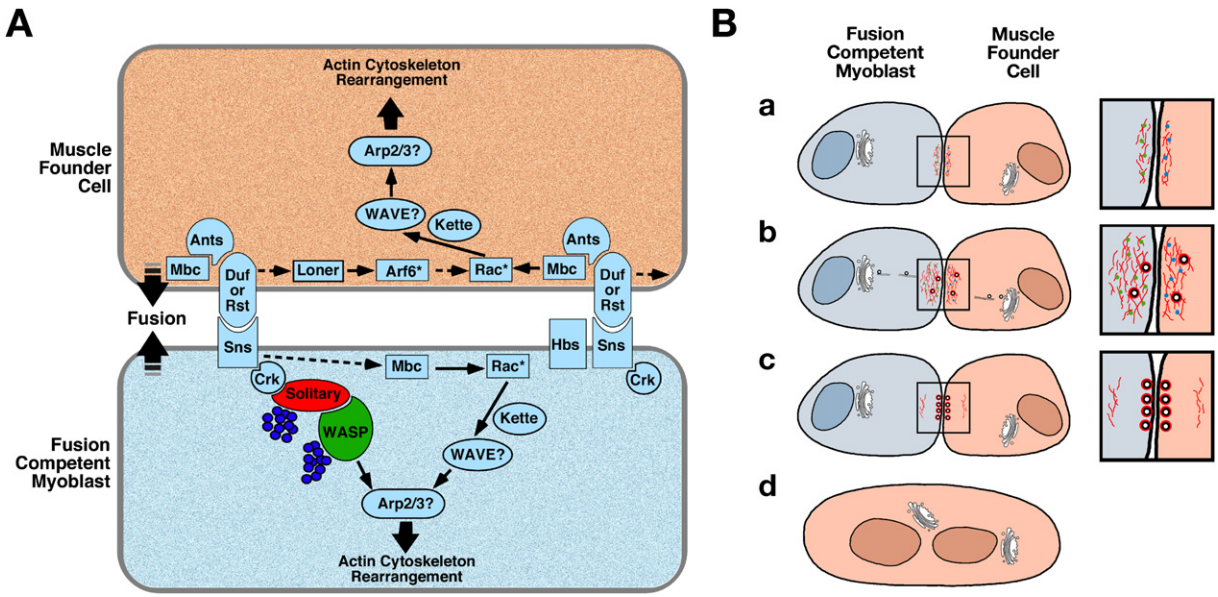

Figure 8. Signal Transduction and the Function of the Actin Cytoskeleton during Myoblast Fusion

(A) A model for signal transduction in fusion-competent cells. We propose that in fusion-competent cells, Sltr is recruited to sites of fusion by Sns, potentially mediated by the adaptor protein Crk. Localization of Sltr to sites of fusion in turn recruits monomeric G-actin (blue balls) and its binding partner WASP, which leads to localized induction of actin polymerization at sites of fusion. The Sns → Crk → Sltr → WASP pathway is likely parallel to the Mbc → Rac → WAVE pathway that may be involved in fusion-competent cell migration and filopodia formation. Note that the involvement of WAVE or Arp2/3 in myoblast fusion is inferred from their relationship with known signaling components.

(B) A model for the function of the actin cytoskeleton in myoblast fusion. A close-up view of the boxed area is shown on the right.

(a) Following myoblast adhesion, the fusion receptors Sns and Duf (not shown in the schematic) recruit the actin polymerization machinery to sites of fusion. This recruitment is mediated by Sltr (green dots) in the fusion-competent cell and Sltr's counterpart, for example, Ants (blue dots), in the founder cell. Actin filaments are shown in red.

(b) Golgi-derived prefusion vesicles move to the cell periphery on microtubules. The F-actin foci at sites of fusion provide directionality for prefusion vesicle trafficking. While passing through the actin-rich foci, prefusion vesicles become coated with actin (red circle on the vesicle).

(c) Prefusion vesicles remain actin coated after reaching the plasma membrane and the actin-rich foci disintegrate.

(d) Once prefusion vesicles release their contents—a fusogen or proteins/chemicals that stimulate a fusogenic activity—plasma membrane fusion is triggered, leading to the formation of a multinucleated syncytium.

any fusion defects (Luo et al., 1994). Future experiments are required to identify the specific WASP activating factor(s) in myoblast fusion.

The Role of the Actin Cytoskeleton in Myoblast Fusion

Myoblast fusion is a multistep process that includes cell recognition, adhesion, alignment, and membrane merger. To initiate the fusion process, fusion-competent cells that reside in a deeper mesodermal layer in the embryo need to migrate and extend filopodia toward founder cells that are in close contact with the ectoderm. Because the actin cytoskeleton is required for both cell migration and filopodia formation (Etienne-Manneville and Hall, 2002), one may predict that the actin cytoskeleton plays a role in these early events of myoblast fusion. Indeed, mutations in *mbc* and *rac*, components of the Mbc → Rac → WAVE pathway, produce a large number of round-shaped fusion-competent cells (Hakeda-Suzuki et al., 2002; Rushton et al., 1995), suggesting a potential defect in myoblast migration and/or filopodia formation.

What we have identified in this study is a novel function of the actin cytoskeleton in a later step during myoblast fusion. This function is mediated by the Crk → Sltr → WASP pathway, which is independent of that of Mbc → Rac → WAVE, as the recruitment of Sltr by the fusion receptor Sns is not affected by either *mbc* or *rac* (Figures 2N and 2O). Using light microscopy, we have observed F-actin-rich foci localized to sites of fusion during myoblast adhesion, raising the possibility that localized actin polymerization at these sites may be functionally important for fusion. We also demonstrate that the F-actin-rich foci are organized by the fusion receptor and actin cytoskeleton regulators, as they are absent in *sns* and *sltr* mutant fusion-competent cells. Taken together, these observations suggest a potential link between the fusion receptor, actin polymerization, and the membrane fusion machinery.

Our EM studies provide further insights into how localized actin polymerization may contribute to myoblast fusion by uncovering a relationship between the actin-rich foci and prefusion vesicles. We found that the prefusion vesicles are of exocytic origin and are transported to the

plasma membrane via the microtubule network (Figures 6E–6F″; Figures S4A–S4B′). Our immuno-EM analyses further revealed two classes of vesicles, one coated with and the other devoid of actin, at different subcellular locations (Figures 6G″, 6G‴, and 6H″). While naked vesicles are farther away from the actin foci, actin-coated vesicles are either within the foci or have reached the plasma membrane (Figures 6G–6H″; Figures S4C–S4D′). That all vesicles at the membrane are actin-coated suggests that they have transited through actin foci and thus become distinct from the naked vesicles. Although we did not follow the trafficking of these vesicles in real time due to the lack of vesicle-specific markers, the "snapshots" provided by the EM analyses are most consistent with a model that actin foci at sites of fusion provide cortical capturing sites for the prefusion vesicles (Figure 8B). This model is further supported by the transient nature of the actin-rich foci, which disintegrate in the cortical region after the prefusion vesicles have paired along the membrane in mature myoblasts. We believe that this model provides a plausible explanation for the mistargeting of vesicles in *sltr* mutant embryos—in the absence of actin foci at the prospective fusion sites, prefusion vesicles are randomly routed to the plasma membrane, resulting in their accumulation between adjacent founder and fusion-competent cells as well as between neighboring fusion-competent cells.

It is intriguing that in mature myoblasts, the prefusion vesicles that have aligned at the plasma membrane are all actin-coated, concurrent with an absence of the actin-rich patches at the cell cortex. Could actin coating of the prefusion vesicles, as well as disintegration of the actin-rich foci in mature myoblasts, play a role in vesicle-membrane fusion? The failure of vesicle-plasma membrane fusion in *sltr* mutant myoblasts with either too little (in fusion-competent cells) or prolonged accumulation of (in founder cells) actin is consistent with this possibility. While definitive answers to these questions await future investigation, it is worth noting that actin is required for yeast vacuole fusion (Eitzen et al., 2002) and that actin has recently been identified as a component of neuronal synaptic vesicles (Takamori et al., 2006).

An important future direction is to identify the biochemical composition of the prefusion vesicles. The involvement of such vesicles in myoblast fusion is not unique to *Drosophila*, as similar vesicles with electron-dense material have been reported in quail myoblast cultures (Lipton and Konigsberg, 1972) and the L6 rat muscle cells (Engel et al., 1985). It is conceivable that these vesicles may deliver an unknown fusogen, or proteins/chemicals that stimulate fusogen activity, to the fusion sites, which ultimately leads to the fusion of apposing cell membranes. Because the actin cytoskeleton has also been implicated in other types of cell-cell fusion events, including fusion of human macrophages (DeFife et al., 1999) and viral-induced cell-cell fusion (Pontow et al., 2004), we speculate that targeted exocytosis of prefusion vesicles might represent a general step in myoblast fusion from *Drosophila* to mammals and perhaps in other cell-cell fusion events as well.

EXPERIMENTAL PROCEDURES

Fly Genetics

The *sltr*^{S1946} mutant allele was isolated in a genetic screen for muscle development (E.H.C., unpublished data). Other fly stocks were obtained from the Bloomington Stock Center except the following: *lmd/TM3, ftz-lacZ* (H. Nguyen); *rac*^{1}*rac*^{2}*/TM3* and *UAS-CD8GFP* (L. Luo); *sns*$^{40\text{-}49}$*/CyO* (R. Renkowitz-Pol); *FRT*^{82B}, *Wasp*^{3}, *e/TM6B* (A. Zelhof and E. Schejter); *rP298-lacZ* (A. Nose); and *rP298-GAL4* (D. Menon).

Rescue crosses were performed by crossing *Twi-GAL4, sltr/CyO, actin-lacZ* with *UAS-sltr, sltr/CyO, actin-lacZ* or *UAS-"sltr mutant," sltr/CyO, actin-lacZ*, in which "*sltr* mutant" represents *sltrΔWH2-1&2*, *sltrΔWH2-1*, *sltrK49Q*, *sltrΔWH2-2*, or *sltrΔWBD*. *Wasp* germline clones were generated using the FLP/FRT system as described (Chou and Perrimon, 1996). For the GFP diffusion assay, *rP298-GAL4; sltr*^{S1946}*/CyO* males were crossed with *sltr*^{S1946}, *UAS-GFP/CyO* females. Mutant embryos were identified with α-Kr staining.

Immunohistochemistry

Antibody staining is described in the Supplemental Data. For staining of F-actin, embryos were fixed and hand devitellinized, followed by incubation with FITC-conjugated phalloidin (1 μg/ml) (Sigma) for 1 hr at room temperature.

For cell staining, S2 cells and differentiated C2C12 cultures were fixed with 4% paraformaldehyde, washed, and stained with the following: mouse α-V5 (1:1000) (Invitrogen), Cy3-conjugated phalloidin (40 nm) (Molecular Probes), and mouse α-skeletal myosin (MY32) (1:200) (Sigma). Nuclei were visualized by staining with Hoechst 33342 (Invitrogen). Secondary FITC-conjugated antibodies were used at 1:200 (Jackson).

Molecular Biology

The molecular lesion of the *sltr*^{S1946} allele was determined by sequencing genomic DNA amplified from homozygous mutant embryos, identified by the lack of GFP expression present on the balancer chromosome. Full-length EST clones of *sltr*, *Wasp*, and *Crk* were obtained from the *Drosophila* Genomics Resource Center.

Constructs for S2 cell transfection, GST pull-down, and phenotypic rescue, as well as RT-PCR analyses for WASP, WIP, and WIRE expression in C2C12 cells, are described in the Supplemental Data.

Biochemistry

GST-Sltr and GST-Crk were expressed and purified according to standard protocols (Pharmacia). For GST pull-down assays, glutathione-Sepharose beads (Amersham) were mixed with an equal volume of GST fusion proteins at a concentration of approximately 3 μg/μl beads. Beads with immobilized proteins were used to pull down G-actin or target proteins from cell lysates.

Detailed procedures for G-actin binding, F-actin cosedimentation, immunoprecipitation, and GST pull-down are described in the Supplemental Data.

Cell Culture and Transfection

S2 or S2R+ cells were grown in *Drosophila* serum-free medium or Schneider's *Drosophila* medium containing 10% fetal bovine serum (FBS), respectively. Cells were transfected using Effectene (Qiagen) according to the manufacturer's instructions.

Mouse C2C12 cells (ATCC) were maintained in Dulbecco's modified Eagle's medium (DMEM) containing 20% FBS. Differentiation was induced at 70% confluency on plates previously coated with 0.1% gelatin by replacing growth media with differentiation media containing DMEM, 2% heat-inactivated horse serum, 10 μg/ml insulin, and 10 μg/ml transferrin (Invitrogen), and analyzed 2 days after induction.

RNA Interference in C2C12 Cells

See the Supplemental Data.

Transmission Electron Microscopy

EM analysis was carried as described by Doberstein et al. (1997). Briefly, embryos were fixed in heptane that had been previously equilibrated with 25% glutaraldehyde/10% acrolein in 0.1 M sodium-cacodylate buffer (pH 7.4). Postfixation with osmium tetroxide and negative staining with 1% uranyl acetate were performed before embedding with EPON (Sigma). Lead staining was done according to Sato (1968) to improve image analysis. Images were acquired on a Philips CM 120 transmission electron microscope.

Immuno-EM

Immuno-EM was carried out as previously described (Tepass, 1996). Briefly, embryos were prefixed for 30 min in a 1:1 mixture of fixation buffer (8% paraformaldehyde and 0.02% glutaraldehyde in 0.1 M sodium phosphate buffer [pH 7.2]) and heptane under vigorous shaking. After hand devitellinization, the anterior 20% of the embryos was cut off to allow antibody access to the interior of the embryo. The embryos were then washed for 15 min in PBS containing 1% normal goat serum, 50 mM glycine, 1 mg/ml BSA, 0.02% sodium azide, and 0.01% saponin, followed by incubation with α-actin mAb (1:100) (clone AC-40; Sigma) for 2 hr at room temperature. Embryos were then incubated with Nanogold α-mouse Fab′ (1:200) (Nanoprobes) for 2 hr, followed by postfixation and silver enhancement. Dehydration, embedding, and sectioning were done as described in transmission electron microscopy, with the exception that no lead staining was performed in order to keep an overall low background.

Supplemental Data

Supplemental Data include five figures, Supplemental Experimental Procedures, and Supplemental References and are available at http://www.developmentalcell.com/cgi/content/full/12/4/571/DC1/.

ACKNOWLEDGMENTS

We are grateful to Eric Olson in whose lab E.H.C. isolated the *sltr* mutant. We thank Drs. S. Abmayr, D. Andrew, M. Frasch, D. Kiehart, L. Luo, D. Menon, H. Nguyen, A. Nose, R. Renkowitz-Pol, M. Ruiz-Gomez, E. Schejter, A. Zelhof, and the Bloomington Stock Center for antibodies and fly stocks; R. Fetter, K. McDonald, and G. Zhang for protocols and advice on electron microscopy; Lauren Parachini for excellent technical assistance; and Drs. Susan Craig, Eric Grote, and Geraldine Seydoux and anonymous reviewers for helpful comments on the manuscript. This work was supported by grants from the National Institutes of Health, the American Heart Association, the Edward Mallinckrodt Jr. Foundation, and the March of Dimes. E.H.C. is a Searle Scholar and a Packard Fellow.

Received: July 26, 2006
Revised: December 4, 2006
Accepted: February 23, 2007
Published: April 9, 2007

REFERENCES

Abmayr, S.M., Balagopalan, L., Galletta, B.J., and Hong, S.J. (2003). Cell and molecular biology of myoblast fusion. Int. Rev. Cytol. *225*, 33–89.

Anton, I.M., and Jones, G.E. (2006). WIP: a multifunctional protein involved in actin cytoskeleton regulation. Eur. J. Cell Biol. *85*, 295–304.

Anton, I.M., de la Fuente, M.A., Sims, T.N., Freeman, S., Ramesh, N., Hartwig, J.H., Dustin, M.L., and Geha, R.S. (2002). WIP deficiency reveals a differential role for WIP and the actin cytoskeleton in T and B cell activation. Immunity *16*, 193–204.

Artero, R.D., Castanon, I., and Baylies, M.K. (2001). The immunoglobulin-like protein Hibris functions as a dose-dependent regulator of myoblast fusion and is differentially controlled by Ras and Notch signaling. Development *128*, 4251–4264.

Ben-Yaacov, S., Le Borgne, R., Abramson, I., Schweisguth, F., and Schejter, E.D. (2001). Wasp, the *Drosophila* Wiskott-Aldrich syndrome gene homologue, is required for cell fate decisions mediated by Notch signaling. J. Cell Biol. *152*, 1–13.

Bour, B.A., Chakravarti, M., West, J.M., and Abmayr, S.M. (2000). *Drosophila* SNS, a member of the immunoglobulin superfamily that is essential for myoblast fusion. Genes Dev. *14*, 1498–1511.

Brugnera, E., Haney, L., Grimsley, C., Lu, M., Walk, S.F., Tosello-Trampont, A.C., Macara, I.G., Madhani, H., Fink, G.R., and Ravichandran, K.S. (2002). Unconventional Rac-GEF activity is mediated through the Dock180-ELMO complex. Nat. Cell Biol. *4*, 574–582.

Carmena, A., Murugasu-Oei, B., Menon, D., Jimenez, F., and Chia, W. (1998). Inscuteable and numb mediate asymmetric muscle progenitor cell divisions during *Drosophila* myogenesis. Genes Dev. *12*, 304–315.

Chen, E.H., and Olson, E.N. (2001). Antisocial, an intracellular adaptor protein, is required for myoblast fusion in *Drosophila*. Dev. Cell *1*, 705–715.

Chen, E.H., and Olson, E.N. (2004). Towards a molecular pathway for myoblast fusion in *Drosophila*. Trends Cell Biol. *14*, 452–460.

Chen, E.H., and Olson, E.N. (2005). Unveiling the mechanisms of cell-cell fusion. Science *308*, 369–373.

Chen, E.H., Pryce, B.A., Tzeng, J.A., Gonzalez, G.A., and Olson, E.N. (2003). Control of myoblast fusion by a guanine nucleotide exchange factor, loner, and its effector ARF6. Cell *114*, 751–762.

Chereau, D., Kerff, F., Graceffa, P., Grabarek, Z., Langsetmo, K., and Dominguez, R. (2005). Actin-bound structures of Wiskott-Aldrich syndrome protein (WASP)-homology domain 2 and the implications for filament assembly. Proc. Natl. Acad. Sci. USA *102*, 16644–16649.

Chou, T.B., and Perrimon, N. (1996). The autosomal FLP-DFS technique for generating germline mosaics in *Drosophila melanogaster*. Genetics *144*, 1673–1679.

DeFife, K.M., Jenney, C.R., Colton, E., and Anderson, J.M. (1999). Disruption of filamentous actin inhibits human macrophage fusion. FASEB J. *13*, 823–832.

Doberstein, S.K., Fetter, R.D., Mehta, A.Y., and Goodman, C.S. (1997). Genetic analysis of myoblast fusion: blown fuse is required for progression beyond the prefusion complex. J. Cell Biol. *136*, 1249–1261.

Duan, H., Skeath, J.B., and Nguyen, H.T. (2001). *Drosophila* Lame duck, a novel member of the Gli superfamily, acts as a key regulator of myogenesis by controlling fusion-competent myoblast development. Development *128*, 4489–4500.

Dworak, H.A., Charles, M.A., Pellerano, L.B., and Sink, H. (2001). Characterization of *Drosophila* hibris, a gene related to human nephrin. Development *128*, 4265–4276.

Eitzen, G., Wang, L., Thorngren, N., and Wickner, W. (2002). Remodeling of organelle-bound actin is required for yeast vacuole fusion. J. Cell Biol. *158*, 669–679.

Engel, L.C., Egar, M.W., and Przybylski, R.J. (1985). Morphological characterization of actively fusing L6 myoblasts. Eur. J. Cell Biol. *39*, 360–365.

Erickson, M.R., Galletta, B.J., and Abmayr, S.M. (1997). *Drosophila* myoblast city encodes a conserved protein that is essential for myoblast fusion, dorsal closure, and cytoskeletal organization. J. Cell Biol. *138*, 589–603.

Etienne-Manneville, S., and Hall, A. (2002). Rho GTPases in cell biology. Nature *420*, 629–635.

Hakeda-Suzuki, S., Ng, J., Tzu, J., Dietzl, G., Sun, Y., Harms, M., Nardine, T., Luo, L., and Dickson, B.J. (2002). Rac function and regulation during *Drosophila* development. Nature *416*, 438–442.

Kawamura, K., Takano, K., Suetsugu, S., Kurisu, S., Yamazaki, D., Miki, H., Takenawa, T., and Endo, T. (2004). N-WASP and WAVE2 acting downstream of phosphatidylinositol 3-kinase are required for

myogenic cell migration induced by hepatocyte growth factor. J. Biol. Chem. *279*, 54862–54871.

Lilly, B., Galewsky, S., Firulli, A.B., Schulz, R.A., and Olson, E.N. (1994). D-MEF2: a MADS box transcription factor expressed in differentiating mesoderm and muscle cell lineages during *Drosophila* embryogenesis. Proc. Natl. Acad. Sci. USA *91*, 5662–5666.

Lipton, B.H., and Konigsberg, I.R. (1972). A fine-structural analysis of the fusion of myogenic cells. J. Cell Biol. *53*, 348–364.

Luo, L., Liao, Y.J., Jan, L.Y., and Jan, Y.N. (1994). Distinct morphogenetic functions of similar small GTPases: *Drosophila* Drac1 is involved in axonal outgrowth and myoblast fusion. Genes Dev. *8*, 1787–1802.

Martinez-Quiles, N., Rohatgi, R., Anton, I.M., Medina, M., Saville, S.P., Miki, H., Yamaguchi, H., Takenawa, T., Hartwig, J.H., Geha, R.S., and Ramesh, N. (2001). WIP regulates N-WASP-mediated actin polymerization and filopodium formation. Nat. Cell Biol. *3*, 484–491.

McDonald, K.L., and Auer, M. (2006). High-pressure freezing, cellular tomography, and structural cell biology. Biotechniques *41*, 137–143.

Menon, S.D., and Chia, W. (2001). *Drosophila* rolling pebbles: a multidomain protein required for myoblast fusion that recruits D-Titin in response to the myoblast attractant Dumbfounded. Dev. Cell *1*, 691–703.

Miki, H., and Takenawa, T. (2003). Regulation of actin dynamics by WASP family proteins. J. Biochem. (Tokyo) *134*, 309–313.

Nguyen, H.T., Bodmer, R., Abmayr, S.M., McDermott, J.C., and Spoerel, N.A. (1994). D-mef2: a *Drosophila* mesoderm-specific MADS box-containing gene with a biphasic expression profile during embryogenesis. Proc. Natl. Acad. Sci. USA *91*, 7520–7524.

Ormo, M., Cubitt, A.B., Kallio, K., Gross, L.A., Tsien, R.Y., and Remington, S.J. (1996). Crystal structure of the *Aequorea victoria* green fluorescent protein. Science *273*, 1392–1395.

Paunola, E., Mattila, P.K., and Lappalainen, P. (2002). WH2 domain: a small, versatile adapter for actin monomers. FEBS Lett. *513*, 92–97.

Pontow, S.E., Heyden, N.V., Wei, S., and Ratner, L. (2004). Actin cytoskeletal reorganizations and coreceptor-mediated activation of rac during human immunodeficiency virus-induced cell fusion. J. Virol. *78*, 7138–7147.

Ramesh, N., Anton, I.M., Hartwig, J.H., and Geha, R.S. (1997). WIP, a protein associated with Wiskott-Aldrich syndrome protein, induces actin polymerization and redistribution in lymphoid cells. Proc. Natl. Acad. Sci. USA *94*, 14671–14676.

Rau, A., Buttgereit, D., Holz, A., Fetter, R., Doberstein, S.K., Paululat, A., Staudt, N., Skeath, J., Michelson, A.M., and Renkawitz-Pohl, R. (2001). rolling pebbles (rols) is required in *Drosophila* muscle precursors for recruitment of myoblasts for fusion. Development *128*, 5061–5073.

Ruiz-Gomez, M., and Bate, M. (1997). Segregation of myogenic lineages in *Drosophila* requires numb. Development *124*, 4857–4866.

Ruiz-Gomez, M., Coutts, N., Price, A., Taylor, M.V., and Bate, M. (2000). *Drosophila* dumbfounded: a myoblast attractant essential for fusion. Cell *102*, 189–198.

Ruiz-Gomez, M., Coutts, N., Suster, M.L., Landgraf, M., and Bate, M. (2002). myoblasts incompetent encodes a zinc finger transcription factor required to specify fusion-competent myoblasts in *Drosophila*. Development *129*, 133–141.

Rushton, E., Drysdale, R., Abmayr, S.M., Michelson, A.M., and Bate, M. (1995). Mutations in a novel gene, myoblast city, provide evidence in support of the founder cell hypothesis for *Drosophila* muscle development. Development *121*, 1979–1988.

Sato, T. (1968). A modified method for lead staining of thin sections. J. Electron Microsc. (Tokyo) *17*, 158–159.

Schroter, R.H., Lier, S., Holz, A., Bogdan, S., Klambt, C., Beck, L., and Renkawitz-Pohl, R. (2004). kette and blown fuse interact genetically during the second fusion step of myogenesis in *Drosophila*. Development *131*, 4501–4509.

Stradal, T.E., and Scita, G. (2006). Protein complexes regulating Arp2/3-mediated actin assembly. Curr. Opin. Cell Biol. *18*, 4–10.

Strunkelnberg, M., Bonengel, B., Moda, L.M., Hertenstein, A., de Couet, H.G., Ramos, R.G., and Fischbach, K.F. (2001). rst and its paralogue kirre act redundantly during embryonic muscle development in *Drosophila*. Development *128*, 4229–4239.

Takamori, S., Holt, M., Stenius, K., Lemke, E.A., Gronborg, M., Riedel, D., Urlaub, H., Schenck, S., Brugger, B., Ringler, P., et al. (2006). Molecular anatomy of a trafficking organelle. Cell *127*, 831–846.

Tepass, U. (1996). Crumbs, a component of the apical membrane, is required for zonula adherens formation in primary epithelia of *Drosophila*. Dev. Biol. *177*, 217–225.

Volkman, B.F., Prehoda, K.E., Scott, J.A., Peterson, F.C., and Lim, W.A. (2002). Structure of the N-WASP EVH1 domain-WIP complex: insight into the molecular basis of Wiskott-Aldrich syndrome. Cell *111*, 565–576.